Electronic Supplementary Information

Exploiting Single-Molecule Magnet of β-diketone Dysprosium Complexes with C_{3v} Symmetry: Suppression Quantum Tunneling of Magnetization

Yanping Dong,[a,b] Pengfei Yan,[a] Xiaoyan Zou,[a] Tianqi Liu,[a] Guangming Li*[a] etal

[a] *Key Laboratory of Functional Inorganic Material Chemistry (MOE), School of Chemistry and Materials Science, Heilongjiang University, No. 74, Xuefu Road, Nangang District, Harbin, Heilongjiang 150080, P. R. China, E-mail: gmli_2000@163.com. Fax: (+86)451-86608458; Tel: (+86)451-86608458*

[b] *Department of Food and Pharmaceutical Engineering, Suihua University, Suihua , Heilongjiang 15206 (P. R. China)*

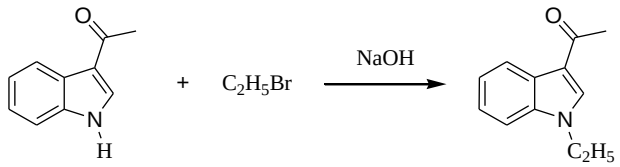

Scheme S1. Synthesis of the EIE

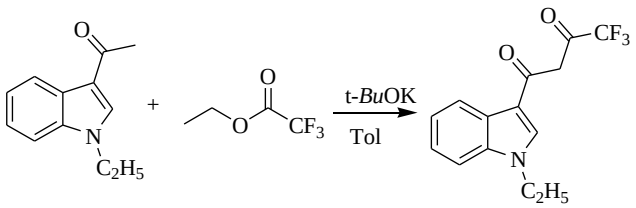

Scheme S2. Synthesis of the EIFD

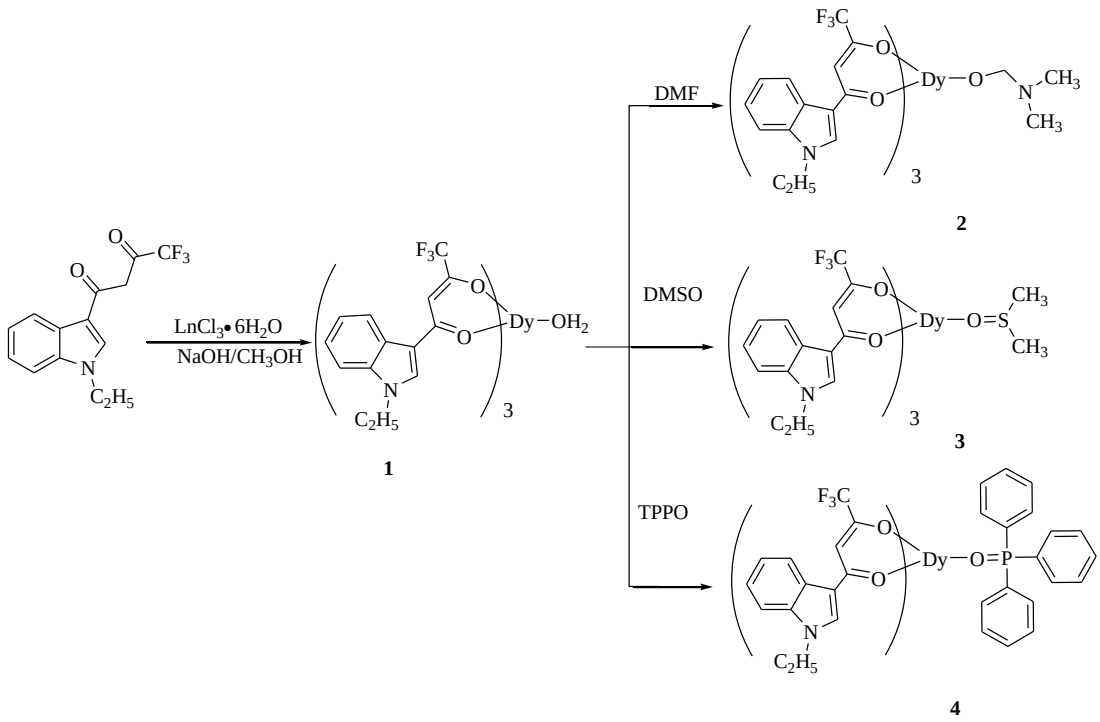

Scheme S3. Synthesis of complexes **1−4**.

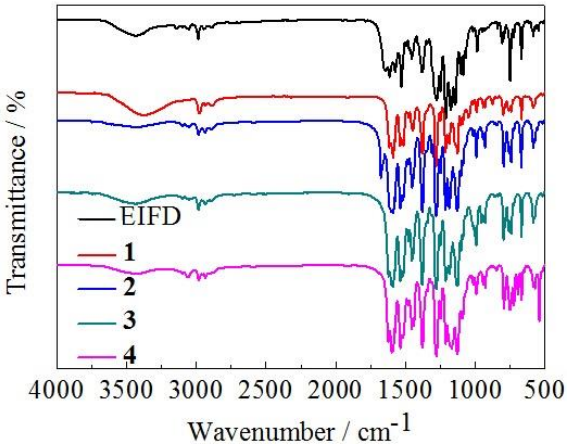

Figure S1. IR spectra of EIFD and complexes **1−4**.

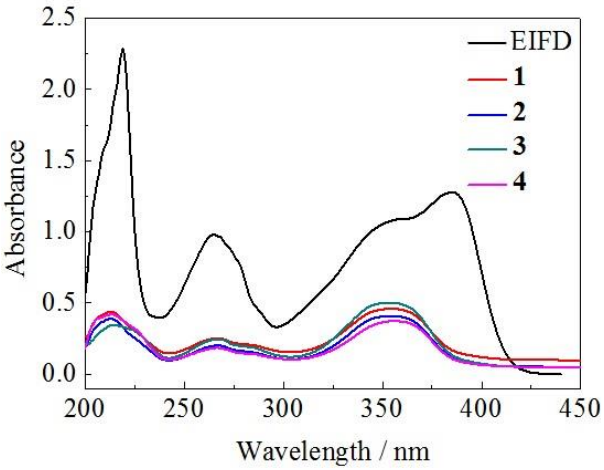

Figure S2. UV absorption spectra of EIFD and complexes **1−4**.

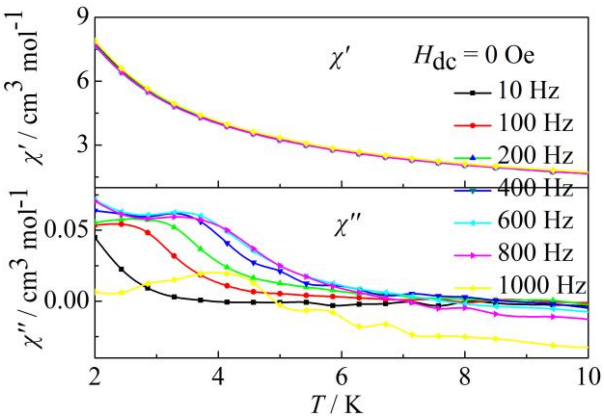

Figure S3. Temperature dependence of the in-phase (χ') and out-of-phase (χ'') ac susceptibility of complex **2** under 0 Oe in the frequency range 10−1000 Hz.

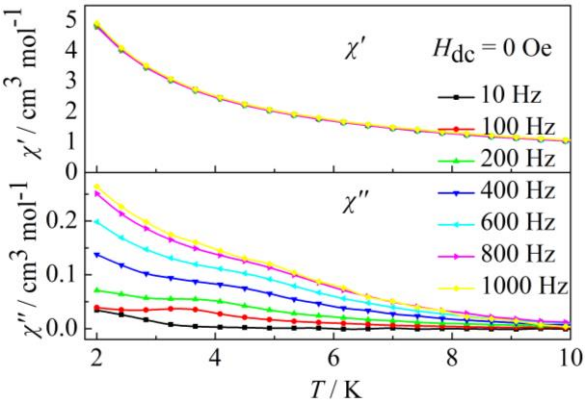

Figure S4. Temperature dependence of the in-phase (χ') and out-of-phase (χ'') ac susceptibility of complex **3** under 0 Oe in the frequency range 10−1000 Hz.

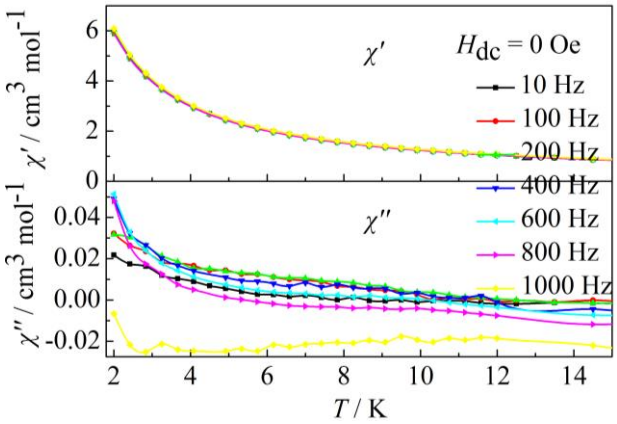

Figure S5. Temperature dependence of the in-phase (χ') and out-of-phase (χ'') ac susceptibility of complex **4** under 0 Oe in the frequency range 10−1000 Hz.

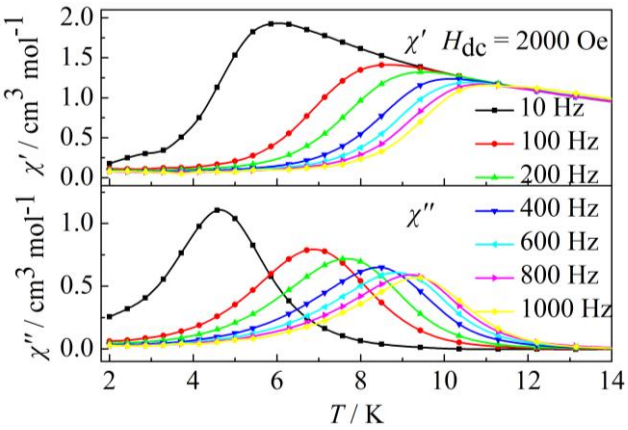

Figure S6. Temperature dependence of the in-phase (χ') and out-of-phase (χ'') ac susceptibility of complex **1** under 2000 Oe in the frequency range 10−1000 Hz.

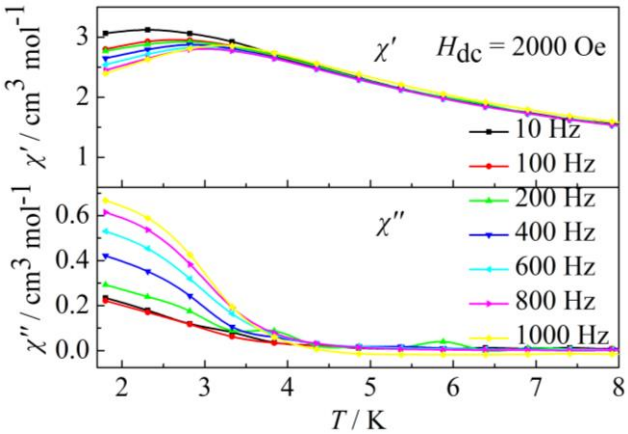

Figure S7. Temperature dependence of the in-phase (χ') and out-of-phase (χ'') ac susceptibility of complex **4** under 2000 Oe in the frequency range 10−1000 Hz.

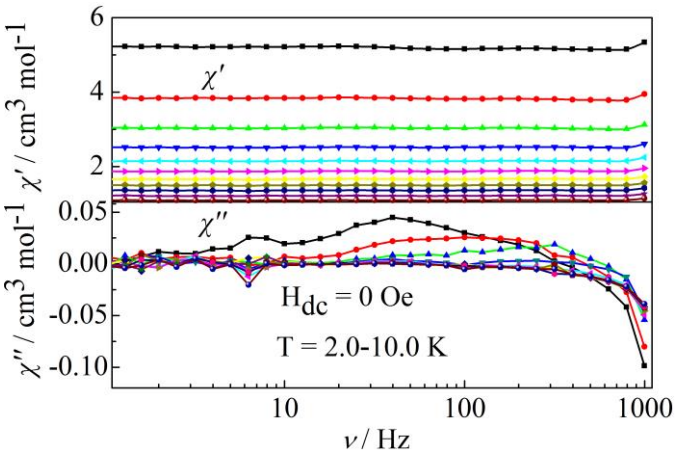

Figure S8. Frequency dependence of the in-phase (χ') and out-of-phase (χ'') ac susceptibility under 0 Oe in the temperature range 2.0−10 K for complex **2**.

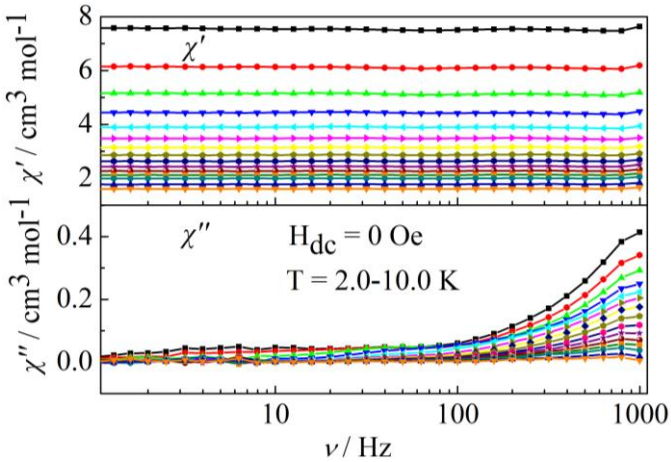

Figure S9. Frequency dependence of the in-phase (χ') and out-of-phase (χ'') ac susceptibility under 0 Oe in the temperature range 2.0−10 K for complex **3**.

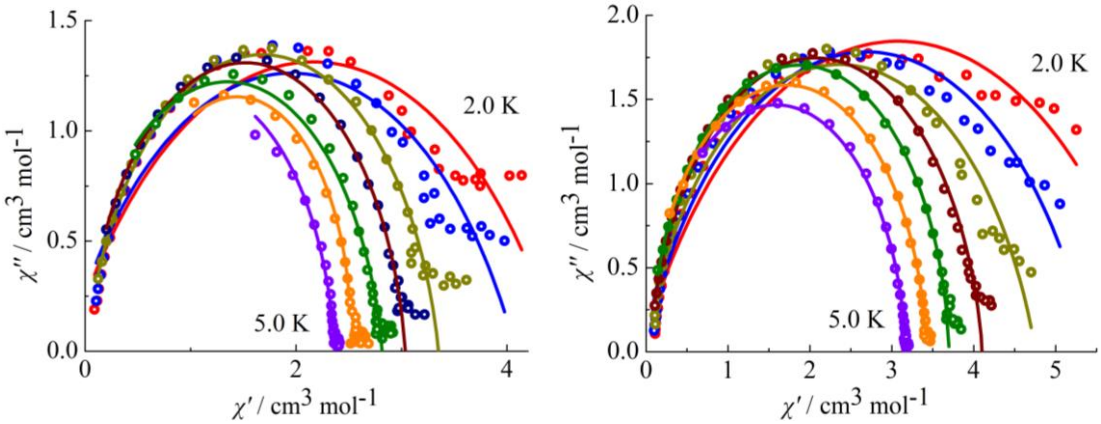

Figure S10. Cole-Cole plots measured at 2.0−5.0 K under 2000 Oe for complexes **2** (left) and **3** (right).

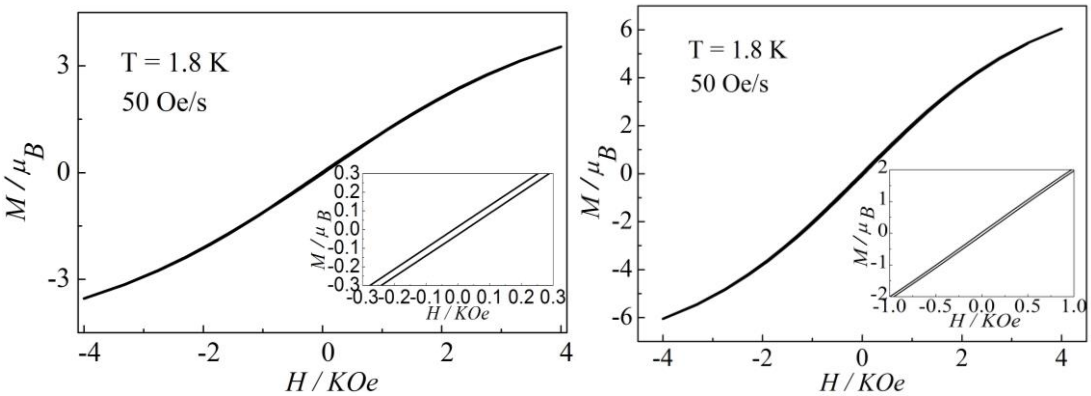

Figure S11. Hysteresis loop for complexes complexes **2** (left) and **3** (right) at 1.8 K.

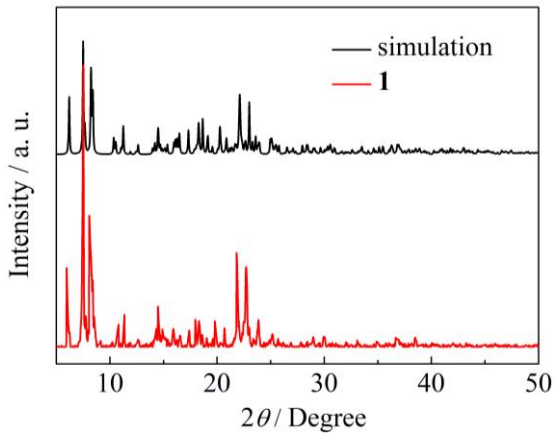

Figure S12. The powder X-Ray diffraction patterns and the simulated patterns of complex **1**.

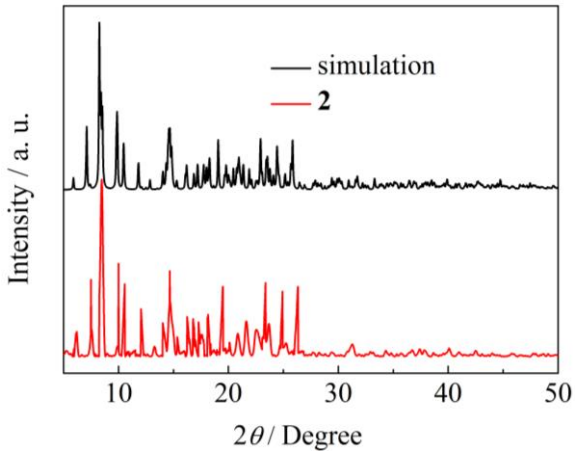

Figure S13. The powder X-Ray diffraction patterns and the simulated patterns of complex **2**.

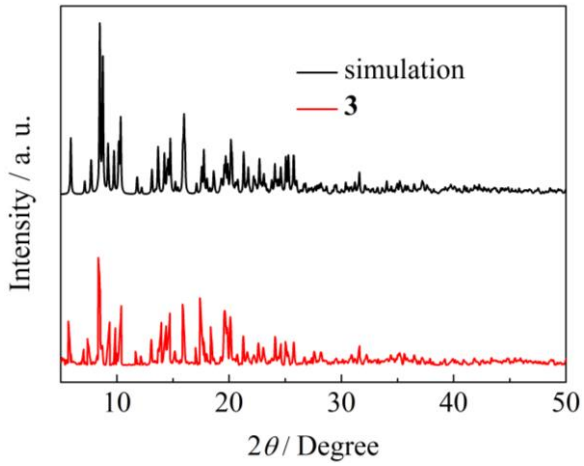

Figure S14. The powder X-Ray diffraction patterns and the simulated patterns of complex **3**.

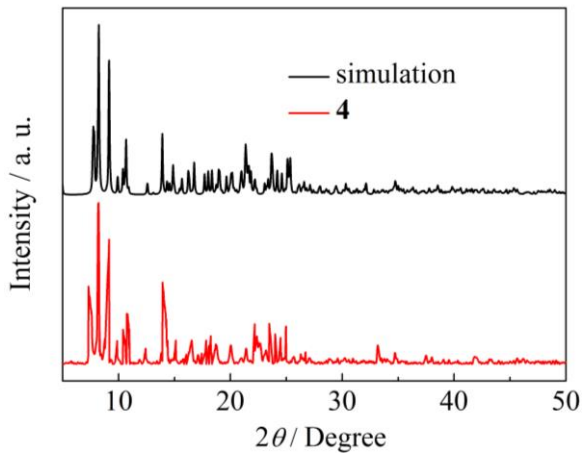

Figure S15. The powder X-Ray diffraction patterns and the simulated patterns of complex **4**.

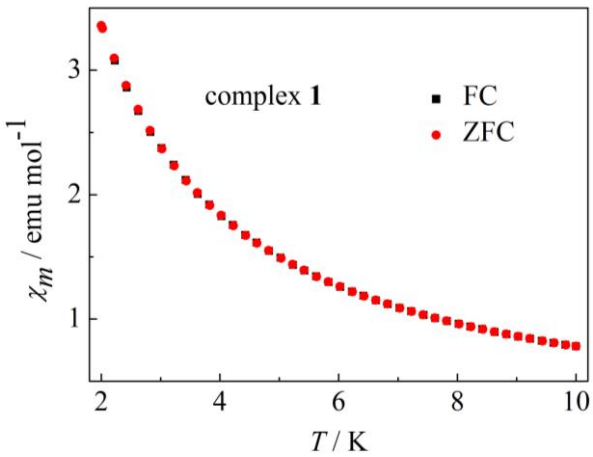

Figure S16. Plots of FC and ZFC magnetization for complex **1** under 1500 Oe.

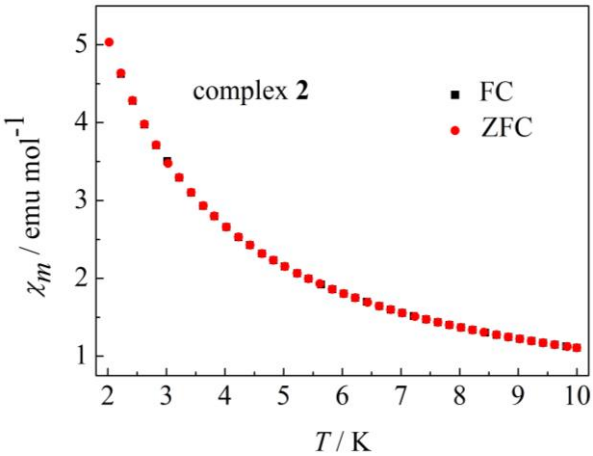

Figure S17. Plots of FC and ZFC magnetization for complex **2** under 1500 Oe.

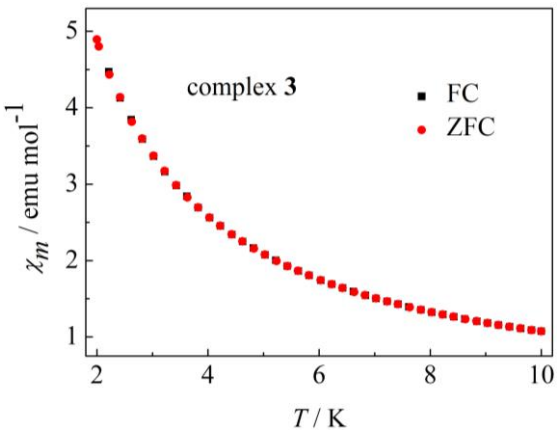

Figure S18. Plots of FC and ZFC magnetization for complex **3** under 1500 Oe.

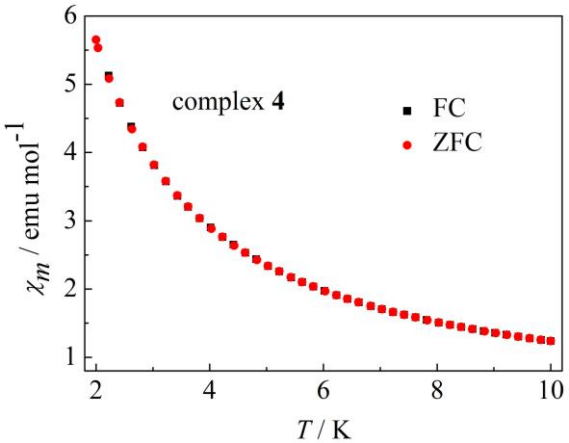

Figure S19. Plots of FC and ZFC magnetization for complex **4** under 1500 Oe.

Table S1. Selected bond lengths and angles for complexes **1**−**4**

1		**2**		3		4	
Dy(1)-O(1)	2.279(3)	Dy(1)-O(3)	2.260(4)	Dy(1)-O(4)	2.268(3)	Dy(2)-O(8)	2.267(3)
Dy(1)-O(2)	2.293(3)	Dy(1)-O(7)	2.289(5)	Dy(1)-O(6)	2.295(3)	Dy(2)-O(11)	2.291(3)
Dy(1)-O(3)	2.292(3)	Dy(1)-O(1)	2.293(5)	Dy(1)-O(7)	2.308(3)	Dy(2)-O(10)	2.312(3)
Dy(1)-O(4)	2.333(3)	Dy(1)-O(4)	2.317(4)	Dy(1)-O(3)	2.312(3)	Dy(2)-O(9)	2.313(3)
Dy(1)-O(5)	2.256(3)	Dy(1)-O(6)	2.320(5)	Dy(1)-O(1)	2.315(3)	Dy(2)-O(14)	2.314(3)
Dy(1)-O(6)	2.358(3)	Dy(1)-O(5)	2.333(5)	Dy(1)-O(2)	2.326(3)	Dy(2)-O(13)	2.318(3)
Dy(1)-O(7)	2.379(3)	Dy(1)-O(2)	2.351(4)	Dy(1)-O(5)	2.337(3)	Dy(2)-O(12)	2.365(3)
O(5)-Dy(1)-O(1)	116.54(12)	O(3)-Dy(1)-O(7)	160.71(19)	O(4)-Dy(1)-O(6)	107.53(11)	O(8)-Dy(2)-O(11)	78.83(11)
O(5)-Dy(1)-O(3)	77.70(12)	O(3)-Dy(1)-O(1)	107.19(18)	O(4)-Dy(1)-O(7)	160.24(12)	O(8)-Dy(2)-O(10)	97.79(12)
O(1)-Dy(1)-O(3)	74.26(12)	O(7)-Dy(1)-O(1)	82.0(2)	O(6)-Dy(1)-O(7)	87.47(12)	O(11)-Dy(2)-O(10)	73.28(11)
O(5)-Dy(1)-O(2)	81.29(11)	O(3)-Dy(1)-O(4)	74.17(16)	O(4)-Dy(1)-O(3)	74.30(10)	O(8)-Dy(2)-O(9)	74.67(10)
O(1)-Dy(1)-O(2)	74.91(11)	O(7)-Dy(1)-O(4)	89.59(18)	O(6)-Dy(1)-O(3)	149.47(11)	O(11)-Dy(2)-O(9)	134.51(11)
O(3)-Dy(1)-O(2)	129.18(11)	O(1)-Dy(1)-O(4)	151.18(18)	O(7)-Dy(1)-O(3)	86.24(12)	O(10)-Dy(2)-O(9)	74.50(12)
O(5)-Dy(1)-O(4)	107.38(11)	O(3)-Dy(1)-O(6)	77.86(17)	O(4)-Dy(1)-O(1)	100.93(12)	O(8)-Dy(2)-O(14)	177.68(10)
O(1)-Dy(1)-O(4)	116.97(11)	O(7)-Dy(1)-O(6)	121.38(19)	O(6)-Dy(1)-O(1)	130.78(11)	O(11)-Dy(2)-O(14)	103.48(11)
O(3)-Dy(1)-O(4)	73.60(11)	O(1)-Dy(1)-O(6)	73.06(18)	O(7)-Dy(1)-O(1)	77.26(12)	O(10)-Dy(2)-O(14)	82.73(11)
O(2)-Dy(1)-O(4)	157.21(12)	O(4)-Dy(1)-O(6)	133.38(18)	O(3)-Dy(1)-O(1)	76.52(11)	O(9)-Dy(2)-O(14)	103.35(10)
O(5)-Dy(1)-O(6)	73.60(11)	O(3)-Dy(1)-O(5)	107.03(19)	O(4)-Dy(1)-O(2)	78.76(11)	O(8)-Dy(2)-O(13)	102.15(11)
O(1)-Dy(1)-O(6)	152.18(12)	O(7)-Dy(1)-O(5)	79.8(2)	O(6)-Dy(1)-O(2)	75.28(10)	O(11)-Dy(2)-O(13)	76.39(11)
O(3)-Dy(1)-O(6)	133.28(11)	O(1)-Dy(1)-O(5)	124.26(18)	O(7)-Dy(1)-O(2)	118.37(12)	O(10)-Dy(2)-O(13)	139.40(11)
O(2)-Dy(1)-O(6)	81.70(10)	O(4)-Dy(1)-O(5)	80.66(17)	O(3)-Dy(1)-O(2)	133.23(11)	O(9)-Dy(2)-O(13)	144.99(11)
O(4)-Dy(1)-O(6)	80.76(11)	O(6)-Dy(1)-O(5)	72.83(17)	O(1)-Dy(1)-O(2)	71.94(10)	O(14)-Dy(2)-O(13)	78.76(11)
O(5)-Dy(1)-O(7)	149.18(11)	O(3)-Dy(1)-O(2)	81.10(18)	O(4)-Dy(1)-O(5)	81.60(11)	O(8)-Dy(2)-O(12)	83.79(11)
O(1)-Dy(1)-O(7)	85.15(12)	O(7)-Dy(1)-O(2)	85.5(2)	O(6)-Dy(1)-O(5)	73.51(10)	O(11)-Dy(2)-O(12)	139.45(11)
O(3)-Dy(1)-O(7)	131.62(11)	O(1)-Dy(1)-O(2)	73.70(16)	O(7)-Dy(1)-O(5)	90.78(12)	O(10)-Dy(2)-O(12)	145.89(11)
O(2)-Dy(1)-O(7)	84.06(11)	O(4)-Dy(1)-O(2)	78.21(16)	O(3)-Dy(1)-O(5)	76.74(11)	O(9)-Dy(2)-O(12)	73.12(11)
O(4)-Dy(1)-O(7)	78.05(11)	O(6)-Dy(1)-O(2)	132.83(17)	O(1)-Dy(1)-O(5)	151.30(10)	O(14)-Dy(2)-O(12)	94.50(10)
O(6)-Dy(1)-O(7)	77.56(11)	O(5)-Dy(1)-O(2)	154.27(17)	O(2)-Dy(1)-O(5)	135.74(10)	O(13)-Dy(2)-O(12)	71.88(11)

Table S2. Fitted parameters of the Cole-Cole plots for complexes **2** and **3** under 2000 Oe

complex **2**				complex **3**			
T/K	χ_S	χ_T	α	T/K	χ_S	χ_T	α
2.0	0.19001	4.01051	0.21160	2.0	0.06007	5.79892	0.28430
2.5	0.19000	3.90001	0.20326	2.5	0.08002	5.10509	0.21764
3.0	0.04027	3.36703	0.13267	3.0	0.08000	4.60020	0.15477
3.5	0.06017	3.10045	0.09833	3.5	0.02951	4.10103	0.09431
4.0	0.00130	2.82126	0.09123	4.0	0.02025	3.77866	0.09004
4.5	0.00212	2.59752	0.09002	4.5	0.02001	3.46758	0.09001
5.0	0.01127	2.39150	0.09163	5.0	0.00572	3.20121	0.09000